# Ballistic Target Tracking Using Range Spread Measurements of a Wideband Radar Seeker

Boyoung Jung
*School of Mechanical and Control Eng.*
*Handong University*
Pohang, South Korea
boyoung@handong.ac.kr

Chan-Seok Lee
*Missile Research Institute*
*Agency for Defense Development*
Deajeon, South Korea
coldstone@add.re.kr

Won-Sang Ra
*School of Mechanical and Control Eng.*
*Handong University*
Pohang, South Korea
wonsang@handong.ac.kr

***Abstract*—This paper deals with the ballistic target tracking problem using range spread measurements. Based on the fact that the range spread measurement distribution can be successfully approximated by the Gaussian mixture model, the problem is formulated in the framework of Gaussian sum filtering. A probabilistic mode merging algorithm is developed to ensure both the computational efficiency and the suboptimal performance. The proposed filter guarantees the operational reliability of the tracking algorithm, since it does not suffer from the degeneracy problem often encountered with the particle filter, which causes target tracking failure. The simulations for a typical ballistic target interception scenario demonstrate the effectiveness and the superior performance of the suggested method over the existing nonlinear filters.**

***Keywords—range spread measurements, high resolution radar, Gaussian mixture, adaptive mode management***

## I. INTRODUCTION

The primary goal of the interceptor in the missile defense system is to effectively neutralize the ballistic target threat by hit-to-kill its warhead. To mitigate the potential for substantial damage in the event of interception failure, precise aimpoint calculation is essential. For this purpose, most interceptors equipped with wideband radar seekers with the range resolution much smaller than the length of a ballistic target (BT). The superior resolution of wideband radar seekers helps to acquire more information about the BT, but paradoxically, the statistical nonlinearity of the range spread measurement makes aim point estimation difficult [1]. To tackle this challenge, it is crucial to develop a practical target tracking algorithm, which is capable of handling the multimodal measurement distribution.

The solutions to the non-Gaussian state estimation problem that have been studied so far can be categorized into sample-based filtering methods and mode-based filtering methods. The sample-based filtering technique is a method of approximating nonlinear probability distribution into a number of discretized samples. Typical examples include grid filters and particle filters (PF). This technique is a numerical approximation of the general solution of Bayesian filtering, and it has the advantage of being very intuitive in its algorithm. However, in BT tracking problems based on a radar seeker with high range resolution, the probability distribution of range measurements consists of several sharp modes. Thus, the target tracking performance of the sample based nonlinear filters could be severely degraded due to degeneracy and sample impoverishment caused by sequential Monte-Carlo sampling during the measurement update process [2-4].

On the contrary, the mode-based filtering technique is based on the Gaussian sum filter (GSF) proposed [5]. This technique approximates the nonlinear statistics of external noise and state estimates into the Gaussian mixture model (GMM), and it has been proven to be the optimal solution for linear systems within the Bayesian framework. Also, this approach has the advantage of being free from the numerical instability issues associated with Monte-Carlo sampling. However, as time goes by, the number of modes of the *a posteriori* probability density function (PDF) increases exponentially during the measurement update process, which may lead to real-time implementation issues due to computational and memory limitations. Therefore, a systematic mode management technique for nonlinear PDFs that can increase computational efficiency without sacrificing state estimation performance needs to be developed.

The mode management techniques have been studied so far using an optimization perspective and a statistical perspective. The optimization-based mode management approach aims to approximate the PDF at each moment into a weighted sum of a prescribed number of Gaussian distributions [6-10]. This method generally considers the number of modes as a design variable. However, in the case of range spread measurements, the improper setting of the mode number may lead to computation waste or a decrease in estimation performance since the shape of the PDF change continuously depending on the aspect angle. On the other hand, probabilistic mode management techniques evaluate the significance of modes probabilistically to perform merging or pruning, which allows them to respond adaptively to changes in the number and shape of PDF modes, more so than optimization-based approaches [5,11]. However, similar to optimization-based methods, they rely on the engineer's heuristics to set threshold values used in mode management, thus sharing the disadvantage of having to repeat the process for performance optimization.

To address the aforementioned issues, this paper proposes a new suboptimal GSF design method that takes into account the statistical characteristics of range spread measurements, adaptively. By focusing on the feature that the variance of range spread measurements obtained from a wideband radar seeker is small enough, we generate mode combination hypotheses for the measurement and its noise distribution, and merge the modes created by a single combination hypothesis to maintain one mode per hypothesis. In this case, we can effectively solve the mode proliferation issue of the conventional GSF and achieve satisfactory state estimation performance. The suboptimality of the proposed filter is analyzed by comparing the unbiasedness of the derived estimates with the ideal GSF. Furthermore, through simulation, we confirm its superiority in computational efficiency compared to existing filters.

The paper is organized as follows. In Section II, we derive the system model for BT tracking and briefly review the characteristics of range spread measurements. In Section III, we introduce how to design the BT tracking filter based on the GSF theory and propose the adaptive mode management methodology for real-time implementation. Simulation results are presented in Section IV. The final section, Section V, presents a summary of the concluding remarks.

## II. System Modeling

### A. Relative Kinematics

Let's consider the engagement geometry on the vertical plane as shown in Fig. 1. In the figure, $(X_I, Z_I)$ represents the inertial axes, $r$ is the relative range between the target and the missile, $\lambda$ is the Line of Sight (LOS) angle, and $\omega = \dot{\lambda}$ denotes the LOS rate in the vertical plane. $(a_m, v_m, \gamma_m)$ and $(a_t, v_t, \gamma_t)$ represent the pitch acceleration, velocity, and flight path angle of the missile and the target, respectively. In this context, the relative velocity can be written as follows.

$$\begin{aligned} \ddot{r} - r\omega^2 &\approx -v_t \sin(\gamma_t - \lambda)\,\dot{\gamma}_t + v_m \sin(\gamma_m - \lambda)\dot{\gamma}_m \\ &= a_t - a_m \end{aligned} \quad (1)$$

In (1), the unknown target acceleration $a_t$ can be modeled using the Singer model as follows [12].

$$\dot{a}_t = -1/\tau \cdot a_t + w \quad (2)$$

where $\tau$ represents the target maneuver time constant, and $w$ is assumed to be zero-mean white noise with variance $q$.

When the continuous-time target dynamics model represented by (1) and (2) is discretized with a sampling interval $T$, the following discrete-time model is obtained.

$$\boldsymbol{x}_k = F\boldsymbol{x}_{k-1} + \boldsymbol{u}_{k-1} + G u_{c,k-1}, \;\; \boldsymbol{u}_{k-1} \sim \mathcal{N}(0, Q_{k-1}) \quad (3)$$

where the subscripts $k$ and $k-1$ denote the time steps. $\boldsymbol{x}$ is the state vector and $u_c$ is the control input provided by the Inertial Navigation Unit (INU) onboard the missile.

$$\boldsymbol{x}_{k-1} \triangleq \begin{bmatrix} r_{k-1} \\ \dot{r}_{k-1} \\ a_{t,k-1} \end{bmatrix}, \;\; \boldsymbol{u}_{k-1} = \begin{bmatrix} 0 \\ 0 \\ w_{k-1} \end{bmatrix}, \;\; u_{c,k-1} = -a_{m,k-1},$$

$$F \triangleq \begin{bmatrix} 1 & T & \frac{T^2}{2} \\ 0 & 1 & T \\ 0 & 0 & 1 \end{bmatrix}, \;\; G \triangleq \begin{bmatrix} \frac{T^2}{2} \\ T \\ 1 \end{bmatrix}, \;\; Q_{k-1} \triangleq q \begin{bmatrix} \frac{T^5}{20} & \frac{T^4}{8} & \frac{T^3}{6} \\ \frac{T^4}{8} & \frac{T^3}{3} & \frac{T^2}{2} \\ \frac{T^3}{6} & \frac{T^2}{2} & T \end{bmatrix}.$$

### B. Range spread measurement model

It is well-known that one of the easiest ways to improve the target detection performance of a wideband radar is to perform the detection process for each range cell [13,14]. Based on the standing assumption that this signal processing strategy is applied, this paper models the range spread measurement distribution.

At time instant $k$, the range spread measurements provided by the wideband radar seeker is described by the following equation.

$$\boldsymbol{z}_k = \mathcal{H}\boldsymbol{x}_k + \boldsymbol{v}_k \quad (4)$$

where

$$\boldsymbol{z}_k \triangleq \begin{bmatrix} z_k^1 \\ \vdots \\ z_k^M \end{bmatrix}, \;\; \mathcal{H} \triangleq \begin{bmatrix} H \\ \vdots \\ H \end{bmatrix} \in \mathbb{R}^{M\times 3}, H \triangleq [1 \;\; 0 \;\; 0], \;\; \boldsymbol{v}_k \triangleq \begin{bmatrix} v_k^1 \\ \vdots \\ v_k^M \end{bmatrix}.$$

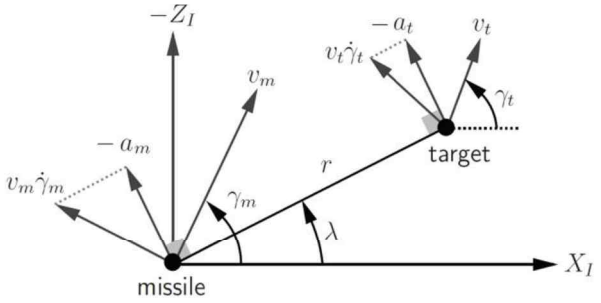


Fig. 1. Engagement geometry in the vertical plane.

Now, let's model the range measurement distribution. We first define the seeker's sum-channel signal power $\mathcal{A}$ as follows.

$$\mathcal{A} = [A(1), \ldots, A(N_r)] \quad (5)$$

where $N_r$ represents the number of range cells, and $A(n)$, the received signal power in the $n$-th range cell.

The equation in relation to the detection threshold $T_h(n)$ for each cell to the probability of false alarm $P_{fa}(n)$ is as follows.

$$T_h(n) = 2\sigma\sqrt{\ln\left(1/P_{fa}(n)\right)} \quad (6)$$

where $\sigma$ denotes the noise standard deviation of the I/Q (in-phase and quadrature) signals. Thus, when $A(n) > T_h(n)$, detection is made in that particular range cell.

Given that the range resolution of the wideband radar seeker is much smaller compared to the length of the target, the scintillation effect in which the received signal power fluctuates can be modeled by Swerling Case 1/2. In this case, the received signal power in the $n$-th range cell is described by the following PDF [14].

$$p_1\big(A(n)\big) = \frac{A(n)}{\sigma^2(1+d(n))} \exp\left(\frac{-A^2(n)}{2\sigma^2(1+d(n))}\right) \quad (7)$$

where $d(n)$ represents the signal-to-noise ratio (SNR) of the $n$-th range cell.

From (6) and (7), the frequency of acquiring the range measurement in the $n$-th range cell. That is, the target detection probability $P_D(n)$, can be calculated as follows.

$$P_D(n) = \int_{T_h(n)}^{\infty} p_s\big(A(n)\big)dA(n) = \exp\left(\frac{-T_h^2(n)}{2\sigma^2(1+d(n))}\right) \quad (8)$$

Therefore, the range measurement noise distribution $p\big(v_r^j\big)$ can be approximated as shown below.

$$p\big(v_k^j\big) \approx P_D(n) / \textstyle\sum_{l=1}^{N_r} P_D(n) \quad (9)$$

In order to verify the validity of the above equation, simulations were conducted to derive the distribution of range measurements. The results are presented in Fig. 2. In the simulation, SNR was assumed as 20 [dB] and $P_{fa} = 10^{-8}$. Under these conditions, the threshold values for detection in each range cell (6) are represented by the blue dotted line. Fig. 3 shows a histogram of the observed power of the target echo

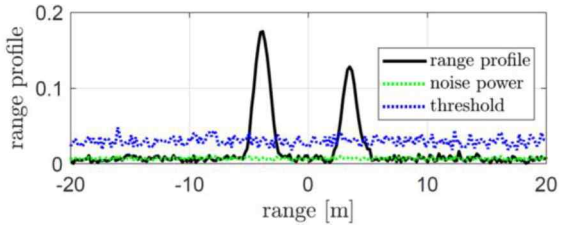


Fig. 2. Example of a target range profile at an aspect angle of 20 degrees.

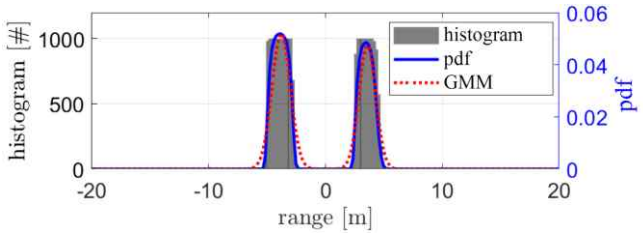


Fig. 3. Histogram and approximated PDF for range spread measurements.

signal and the actual distribution of the range measurement noise. As can be seen in the figure, the range measurement noise distribution (9) can be written as a Gaussian mixture.

$$p(v_k^j) = \sum_{i=1}^{N_v} \gamma_k^{(i)} \mathcal{M}_{v,k}^{(i)} \tag{10}$$

where $\mathcal{M}_{v,k}^{(i)} \triangleq \mathcal{N}(v_k^j; \Delta r_k^{(i)}, (\sigma_{r,k}^{(i)})^2)$ indicates that the random variable $v_k^j$ follows the Gaussian distribution with the mean $\Delta r_k^{(i)}$ and standard deviation $\sigma_{r,k}^{(i)}$. $N_v$ is the number of modes (or the number of Gaussian distributions) that compose the GMM.

If in (4) the range spread measurement noise $v_k^j$ is independent from one another, then the PDF of the measurement noise $\boldsymbol{v}_k$ can be written as follows using (10).

$$p(\boldsymbol{v}_k) = \prod_{j=1}^{M} p(v_k^j) = \prod_{j=1}^{M} \sum_{i=1}^{N_v} \gamma_k^{(i)} \mathcal{M}_{v,k}^{(i)} \tag{11}$$

As can be seen in the above equation, the mode of $p(\boldsymbol{v}_k)$ is determined by the combination of modes in the measurements and the measurement noise distribution, yielding a total of $L = (N_v)^M$ modes.

To simplify the mathematical derivation, if the mode combination of the $l$-th measurement noise distribution is defined as $\varphi_l$, $\varphi_l$ is shown as $M$ tuples as shown in the following equation.

$$\varphi_l \in \Phi^M, \; l = 1,2,\dots,L \tag{12}$$

Here, when $\Phi = \{1,\dots,N_v\}$, $\Phi^M = \{(n_1,\cdots,n_M) | n_i \in \Phi, i = 1,\dots,M\}$ is implied.

To specify, let's examine an example of the combinations of the measurement-measurement noise distribution modes in the case when $N_v = 2$ and $M = 3$ as presented in Table 1. In the case where the combination is $\varphi_l = (1,1,1)$, the mode $\mathcal{M}_{v,k}(\varphi_1)$ and weight $\Gamma_k(\varphi_1)$ are calculated as shown in (11).

$$\mathcal{M}_{v,k}(\varphi_1) = \mathcal{M}_{v,k}^{(1)} \mathcal{M}_{v,k}^{(1)} \mathcal{M}_{v,k}^{(1)}, \;\; \Gamma_k(\varphi_1) = \left(\gamma_k^{(1)}\right)^3 \tag{13}$$

As shown in the table, the total number of modes $\mathcal{M}_{v,k}(\cdot)$ and weights $\Gamma_k(\cdot)$ of $p(\boldsymbol{v}_k)$ is $L = 2^3$, and are all calculated using the exact method as in (13).

Generalizing (13) allows us to rewrite (11) as shown below.

TABLE I. AN EXAMPLE OF THE MODE COMBINATIONS ($N_v = 2, M = 3$).

| | $\varphi_1 = (1,1,1)$ | $\varphi_2 = (1,1,2)$ | ⋯ | $\varphi_8 = (2,2,2)$ |
|---|---|---|---|---|
| $z_k^1$ | $\mathcal{M}_{v,k}^{(1)}$ | $\mathcal{M}_{v,k}^{(1)}$ | ⋯ | $\mathcal{M}_{v,k}^{(2)}$ |
| $z_k^2$ | $\mathcal{M}_{v,k}^{(1)}$ | $\mathcal{M}_{v,k}^{(1)}$ | ⋯ | $\mathcal{M}_{v,k}^{(2)}$ |
| $z_k^3$ | $\mathcal{M}_{v,k}^{(1)}$ | $\mathcal{M}_{v,k}^{(2)}$ | ⋯ | $\mathcal{M}_{v,k}^{(2)}$ |

$$p(\boldsymbol{v}_k) = \sum_{l=1}^{L} \Gamma_k(\varphi_l) \mathcal{M}_{v,k}(\varphi_l), \;\; \sum_{l=1}^{L} \Gamma_k(\varphi_l) = 1 \tag{14}$$

where $\mathcal{M}_{v,k}(\varphi_l) = \mathcal{N}(v_k; b_k(\varphi_l), \Sigma_k(\varphi_l))$ is implied. The mean $b_k(\varphi_l) \in \mathbb{R}^{M\times 1}$ and variance $\Sigma_k(\varphi_l) \in \mathbb{R}^{M\times M}$ of weight $\Gamma_k(\varphi_l)$ and $\mathcal{M}_{v,k}(\varphi_l)$ is defined as follows.

$$b_k(\varphi_l) = \begin{bmatrix} \Delta r_k^{(\varphi_l(1))} \\ \vdots \\ \Delta r_k^{(\varphi_l(M))} \end{bmatrix}, \; \Sigma_k(\varphi_l) = \begin{bmatrix} \sigma_{r,k}^{(\varphi_l(1))} & \cdots & 0 \\ \vdots & \ddots & \vdots \\ 0 & \cdots & \sigma_{r,k}^{(\varphi_l(M))} \end{bmatrix}^2,$$

$$\Gamma_k(\varphi_l) = \prod_{j=1}^{M} \gamma_k^{(\varphi_l(j))}.$$

## III. SUBOPTIMAL GAUSSIAN SUM FILTERING APPROACH TO BALLISTIC TARGET TRACKING

### A. Problem Formulation

The previously derived (3) and (4) are considered as the system model for target tracking using range spread measurements.

$$\begin{cases} \boldsymbol{x}_k = F\boldsymbol{x}_{k-1} + \boldsymbol{u}_{k-1} + Gu_{c,k-1} \\ \boldsymbol{z}_k = \mathcal{H}\boldsymbol{x}_k + \boldsymbol{v}_k \end{cases} \tag{15}$$

The PDFs of the process noise $\boldsymbol{u}_{k-1}$ and the measurement noise $\boldsymbol{v}_k$ are described by (3) and (14). Rewriting them gives the following:

$$p(\boldsymbol{u}_{k-1}) = \mathcal{N}(\boldsymbol{u}_{k-1}; \boldsymbol{0}, Q_{k-1})$$

$$p(\boldsymbol{v}_k) = \sum_{l=1}^{L_k} \Gamma_k(\varphi_l) \mathcal{M}_{v,k}(\varphi_l), \;\; \sum_{l=1}^{L_k} \Gamma_k(\varphi_l) = 1.$$

Thus, the state estimation problem for the system model (15) is calculating the *a posteriori* PDF of the state vector $\boldsymbol{x}_k$ using the non-Gaussian range spread measurements $\boldsymbol{z}_k$. If we denote the cumulative range spread measurements up to time $k$ as $Z^k = \{z_1,\dots,z_k\}$, then the *a priori* PDF and the *a posteriori* PDF of $\boldsymbol{x}_k$ are computed according to Bayes' rule and the Law of Total Probability as follows.

$$p(\boldsymbol{x}_k | Z^{k-1}) = \int p(\boldsymbol{x}_k | \boldsymbol{x}_{k-1}) \, p(\boldsymbol{x}_{k-1} | Z^{k-1}) d\boldsymbol{x}_{k-1} \tag{16}$$

$$p(\boldsymbol{x}_k | Z^k) = \frac{p(\boldsymbol{z}_k | \boldsymbol{x}_k) p(\boldsymbol{x}_k | Z^{k-1})}{p(\boldsymbol{z}_k | Z^{k-1})} \tag{17}$$

In the case of non-Gaussian distribution, one common solution to compute (16) and (17) is the particle filter (PF), which is based on Monte-Carlo sampling. However, PF is known to frequently encounter degeneracy problems, particularly when the variance of the measurement noise is small. Consequently, when the measurement distribution is composed of modes with very sharp shapes, it becomes difficult to ensure the operational stability of the tracking filter.

As a solution to the problems mentioned above, the application of the GSF theory can be considered. This is because, from the theoretical perspective, the GSF is the Bayesian optimal estimator for the state estimation problem of linear systems when the PDFs of the state vector and measurements are described by GMMs. The Gaussian sum filtering process is summarized as follows [11].

*1) Initialization*

At time $k = 0$, the initial probability distribution of the state vector $x_0$ is assumed to be modeled by a GMM, composed of $\widehat{N}_0$ modes.

$$p(x_0) = p(x_0|Z^0) = \sum_{i=1}^{\widehat{N}_0} \hat{\pi}_0^{(i)} \widehat{\mathcal{M}}_0^{(i)} \tag{18}$$

where $\widehat{\mathcal{M}}_0^{(i)} = \mathcal{N}\left(x_0; \hat{x}_0^{(i)}, \hat{P}_0^{(i)}\right)$ represents the $i$-th mode of the PDF for $x_0$, and $\hat{\pi}_0^{(i)}$ is the weight for the $i$-th mode, satisfying $\sum_{i=1}^{\widehat{N}_0} \hat{\pi}_0^{(i)} = 1$.

*2) System propagation*

In (15), since the process noise is assumed to be zero-mean white Gaussian noise, the number of modes in the state vector's PDF does not change during time propagation. Therefore, the *a priori* PDF at time $k$ can be written as follows.

$$p(x_k|Z^{k-1}) = \sum_{i=1}^{\overline{N}_k} \bar{\pi}_k^{(i)} \overline{\mathcal{M}}_k^{(i)} \tag{19}$$

where $\overline{N}_k$ is the number of modes in the *a priori* PDF at time $k$, and $\overline{\mathcal{M}}_k^{(i)} = \mathcal{N}\left(x_k; \bar{x}_k^{(i)}, \bar{P}_k^{(i)}\right)$ and $\bar{\pi}_k^{(i)}$ represent the $i$-th mode and weight, respectively.

The mean $\bar{x}_k^{(i)}$ and covariance matrix $\bar{P}_k^{(i)}$ of $\overline{\mathcal{M}}_k^{(i)}$ are obtained by updating the mean $\hat{x}_{k-1}^{(i)}$ and covariance matrix $\hat{P}_{k-1}^{(i)}$ of the $i$-th mode of the *a posteriori* PDF at time $k-1$.

$$\bar{x}_k^{(i)} = F\hat{x}_{k-1}^{(i)} + Gu_{c,k-1} \tag{20}$$

$$\bar{P}_k^{(i)} = F\hat{P}_{k-1}^{(i)}F^T + Q_{k-1} \tag{21}$$

$$\bar{\pi}_k^{(i)} = \hat{\pi}_{k-1}^{(i)} \tag{22}$$

The number of modes is maintained at $\overline{N}_k = \widehat{N}_{k-1}$.

*3) Measurement update*

The *a posteriori* PDF at time $k$ is calculated by taking a weighted sum of the results of the measurement update for each mode of the *a priori* PDF (19) and each mode of the measurement noise PDF (14).

$$p(x_k|Z^k) = \sum_{i=1}^{\overline{N}_k} \sum_{l=1}^{L_k} \hat{\pi}_k^{(il)} \widehat{\mathcal{M}}_k^{(il)} \tag{23}$$

where $\widehat{\mathcal{M}}_k^{(il)} = \mathcal{N}\left(x_k; \hat{x}_k^{(il)}, \hat{P}_k^{(il)}\right)$ is the mode derived from the combination of $\overline{\mathcal{M}}_k^{(i)}$ in (19) and $\mathcal{M}_{v,k}(\varphi_l)$ in (14). The mean $\hat{x}_k^{(il)}$ and covariance matrix $\hat{P}_k^{(il)}$ are calculated as follows.

$$\eta_k^{(il)} = z_k - \mathcal{H}\bar{x}_k^{(i)} - b_k(\varphi_l) \tag{24}$$

$$S_k^{(il)} = \mathcal{H}\bar{P}_k^{(i)}\mathcal{H}^T + \Sigma_k(\varphi_l) \tag{25}$$

$$W_k^{(il)} = \bar{P}_k^{(i)}\mathcal{H}^T\left(S_k^{(il)}\right)^{-1} \tag{26}$$

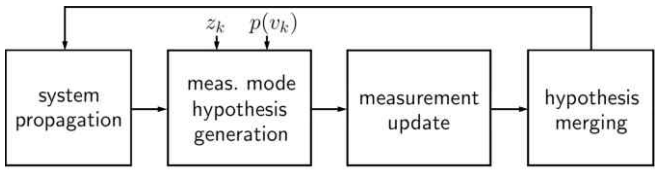


Fig. 4. The structure of the proposed GSF.

$$\hat{x}_k^{(il)} = \bar{x}_k^{(i)} + W_k^{(il)}\eta_k^{(il)} \tag{27}$$

$$\hat{P}_k^{(il)} = \bar{P}_k^{(i)} + W_k^{(il)}\mathcal{H}\bar{P}_k^{(i)} \tag{28}$$

$$\hat{\pi}_k^{(il)} = \frac{1}{C}\bar{\pi}_k^{(i)}\Gamma_k(\varphi_l)\mathcal{N}\left(\eta_k^{(il)}; 0, S_k^{(il)}\right) \tag{29}$$

where $C = \sum_{i=1}^{\overline{N}_k}\sum_{l=1}^{L_k} \hat{\pi}_k^{(il)}$ is the normalization constant.

If the state estimates are computed recursively according to (18)~(29), the number of modes in the *a posteriori* PDF will increase exponentially as follows.

$$\widehat{N}_k = N_0 \times \prod_{i=1}^{k} L_i \tag{30}$$

Therefore, to practically implement the GSF, a separate algorithm is needed to prevent the divergence of the number of modes in the *a posteriori* PDF.

### *B. Adaptive Mode Management for Filter Implementation*

In order to implement the GSF in real-time, an algorithm that adequately preserves the shape of the *a posteriori* PDF and suppresses the divergence of the number of modes is needed. As detailed earlier, the range spread measurements are modeled by a GMM with multiple modes. Notably, each mode of the mentioned GMM has a considerably small variance. Therefore, there is a tendency for the modes of the *a priori* PDF to move very quickly towards the measurements during the measurement update process of GSF. As the number of measurements acquired by the seeker increases, this phenomenon becomes more pronounced. Taking into account the high-resolution traits, this paper defines the hypothesis on the mode combinations derived from the oriented measurement noise PDF of the range spread measurement. Following this hypothesis, the paper designs a suboptimal GSF algorithm that merges the updated modes into one mode.

The structure of the proposed GSF is as depicted in Fig. 4. First, the system propagation in accordance to (19) is performed, and when the range spread measurement $z_k$ is acquired, the mode combination hypothesis $\{\varphi_l\}_{l=1}^{L_k}$ for the measurement noise PDF $p(\boldsymbol{v}_k)$ defined in (12) are generated. Subsequently, measurement updates are made according to the generated measurement noise distribution mode combination hypothesis. And the mode merging is performed to suppress the divergence in the number of modes based on the same mode combination hypothesis.

Fig. 5 demonstrates how the proposed adaptive mode merging technique operates during the filtering process. As shown in the picture, the proposed technique merges the *a posteriori* PDF mode into one, preventing an exponential increase in the number of modes. At time $k$, the number of modes $\overline{N}_k$ in the *a priori* PDF is identical to the number of modes $L_{k-1}$ in the measurement noise distribution of the range spread measurement at time $k-1$. The mean, variance,

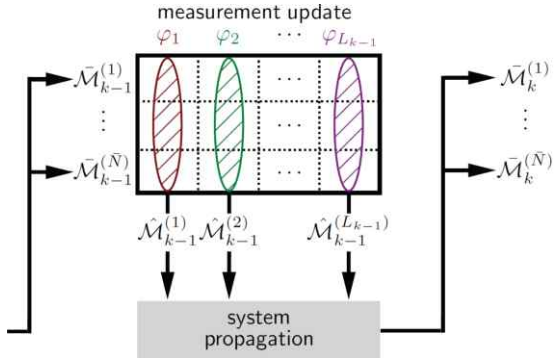


Fig. 5. Adaptive mode management for the proposed GSF.

and weight of the merged *a posteriori* PDF mode $\widehat{\mathcal{M}}_{f,k}^{(l)}$ are calculated as follows.

$$\hat{x}_{f,k}^{(l)} = \sum_{i=1}^{\bar{N}_k} \frac{1}{\hat{\pi}_{f,k}^{(l)}} \hat{\pi}_k^{(il)} \hat{x}_k^{(il)}, \quad \hat{\pi}_{f,k}^{(l)} = \sum_{i=1}^{\bar{N}_k} \hat{\pi}_k^{(il)} \tag{31}$$

$$\hat{P}_{f,k}^{(l)} = \sum_{i=1}^{\bar{N}_k} \frac{1}{\hat{\pi}_{f,k}^{(l)}} \hat{\pi}_k^{(il)} \left(\hat{x}_k^{(il)} - \hat{x}_{f,k}^{(l)}\right)\left(\hat{x}_k^{(il)} - \hat{x}_{f,k}^{(l)}\right)^T \tag{32}$$

The state estimates and estimation error variance of the proposed GSF can be written as the first and second moments.

$$\hat{x}_k = \sum_{j_k=1}^{N_v} \hat{\pi}_{f,k}^{j_k} \hat{x}_{f,k}^{j_k} \tag{33}$$

$$\hat{p}_k = \sum_{j_k=1}^{N_v} \hat{\pi}_{f,k}^{j_k} \left[\hat{p}_{f,k}^{j_k} + \left(\hat{x}_k^{j_k} - \hat{x}_k\right)^2\right] \tag{34}$$

### C. Effectiveness of Adaptive Mode Management

Let's examine the impact of the aforementioned mode management method regarding the estimation error mean of the GSF. For analytical convenience, the one-dimensional linear measurement model where $M = 1,\ H = 1$, and $\boldsymbol{x} \in \mathbb{R}$ in (4).

$$z_k = x_k + v_k,\ p(v_k) = \sum_{j_k=1}^{N_v} \gamma_k^{j_k} \mathcal{N}\left(v_k; b_k^{j_k}, r_k^{j_k}\right) \tag{35}$$

While the ideal GSF is impossible to implement in practice, it can be used as a benchmark to evaluate the performance limitations and suboptimality of the suboptimal GSF with added mode management as it provides a theoretical optimal solution. To do this, the following result was obtained by calculating the mean of the ideal GSF's stats estimation error $\epsilon_k^{opt}$. Here, the PDF of the state variable $x$ is assumed to be $p(x) = \mathcal{N}(x; \bar{x}, \bar{p})$.

$$E\left\{\epsilon_k^{opt}\right\} = 0 \tag{36}$$

The proof for the above expression is as follows. By using $k$ measurements $Z^k = \{z_1, \cdots, z_k\}$, let's represent the PDF of the updated state $x$ using the ideal GSF as a GMM.

$$p(x|Z^k) \triangleq \sum_{i_k=1}^{\bar{N}_k} \hat{\pi}_k^{i_k} \mathcal{N}\left(x; \hat{x}_k^{i_k}, \hat{p}_k^{i_k}\right) \tag{37}$$

The mean and variance of the multi-modal PDF in (37) are as follows.

$$\hat{x}_k^{opt} \triangleq E\{x|Z^k\} = \sum_{i_k=1}^{\bar{N}_k} \hat{\pi}_k^{i_k} \hat{x}_k^{i_k} \tag{38}$$

$$\hat{p}_k^{opt} \triangleq var\{x|Z^k\} = \sum_{i_k=1}^{\bar{N}_k} \hat{\pi}_k^{i_k} \left[\hat{p}_k^{i_k} + \left(\hat{x}_k^{i_k} - \hat{x}_k^{opt}\right)^2\right] \tag{39}$$

If we define (38) as the estimates of the ideal GSF, then the following properties are satisfied for the estimation error $\epsilon_k^{opt} \triangleq x - \hat{x}_k^{opt}$.

$$\hat{x}_k^{opt} \triangleq \int_{-\infty}^{\infty} \hat{x}_k^{opt} p(Z^k) dZ^k \tag{40}$$

That is

$$\hat{x}_k^{opt} = \int_{-\infty}^{\infty} \sum_{i_k=1}^{\bar{N}_k} \hat{\pi}_k^{i_k} \hat{x}_k^{i_k} p(Z^k) dZ^k \ .$$

By substituting (37) into (40), we get the following result.

$$E\left\{\hat{x}_k^{opt}\right\} = \int_{-\infty}^{\infty} \sum_{j_k=1}^{N_v} \sum_{i_{k-1}=1}^{\bar{N}_{k-1}} \gamma_k^{j_k} \hat{\pi}_{k-1}^{j_{k-1}} \times \mathcal{N}\left(\eta_k^{i_{k-1} j_k}; 0, S_k^{i_{k-1} j_k}\right) \hat{x}_k^{i_{k-1} j_k} p(Z^{k-1}) dZ^k \tag{41}$$

By utilizing the key property $\int_{-\infty}^{\infty} xN(x; 0, \sigma^2)dx = 0$ of the Gaussian distribution $N(x; 0, \sigma^2)$, and substituting (38) into the above equation,

$$E\left\{\hat{x}_k^{opt}\right\} = \int_{-\infty}^{\infty} \sum_{i_k=1}^{\bar{N}_{k-1}} \hat{\pi}_{k-1}^{j_{k-1}} \hat{x}_k^{i_{k-1}} p(Z^{k-1}) dZ^{k-1} \tag{42}$$

That is $E\left\{\hat{x}_k^{opt}\right\} = E\left\{\hat{x}_{k-1}^{opt}\right\} = \cdots = E\left\{\hat{x}_0^{opt}\right\}$. Since $\hat{x}_0^{opt} \triangleq E\{x|Z^0\} = E\{x\} = \bar{x}$ is implied, (36) is true.

In the same manner, it can be mathematically verified for the sub-optimal GSF's state estimation error $\epsilon_k \triangleq x - \hat{x}_k$ that the following is satisfied.

$$E\{\epsilon_k\} = 0 \tag{43}$$

For reference, in BT tracking scenarios with a wideband radar seeker, the measurement noise distribution typically has an average of two modes due to the main scattering points at the warhead and tail, and the detections provided after CFAR (Constant False Alarm Rate) processing usually comprises around three modes. Each mode's variance is relatively small compared to the estimation error variance. Therefore, we can expect the suboptimal GSF to achieve tracking performance comparable to the theoretically optimal but unimplementable ideal GSF.

## IV. Simulation Results

To verify the usefulness of the proposed sub-optimal GSF, a simulation was performed for the maneuvering BT engagement scenario depicted in Fig. 6. In the scenario, it is assumed that the BT performs a left turn/pull-up maneuver and then, at 22.35 seconds, abruptly changes the turn direction to the right. The relative range is as shown in Fig. 7.

Based on the center of the 9-meter-long BT, an average of two range spread measurements were generated at both ends of the warhead and the tail of the BT. It is assumed that the measurement noise is modeled by the GMM in which the maximum value of the mode's mean based on the center of the BT is $\left(\Delta r_{max}^{(1)}, \Delta r_{max}^{(2)}\right) = (-4.5, 4.5)[m]$, the standard deviation is $\left(\sigma_r^{(1)}, \sigma_r^{(2)}\right) = (1.0, 0.3)[m]$, and the weight is $\left(\gamma^{(1)}, \gamma^{(2)}\right) = (0.7, 0.3)$. Under these conditions, an example of single-run range spread measurements calculated according to the aspect angle between the BT and missile for the scenario

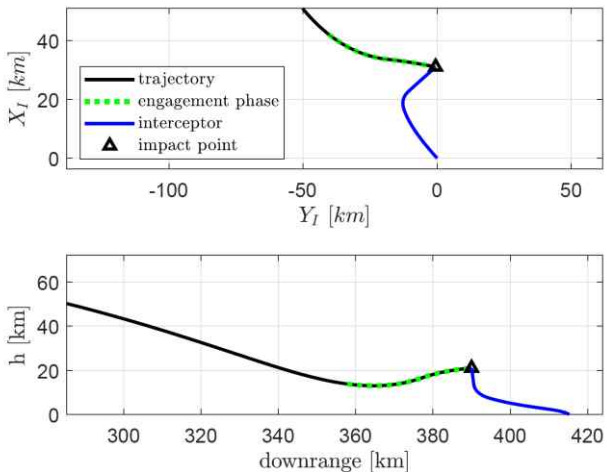


Fig. 6. Maneuvering ballistic target horizontal-vertical trajectory.

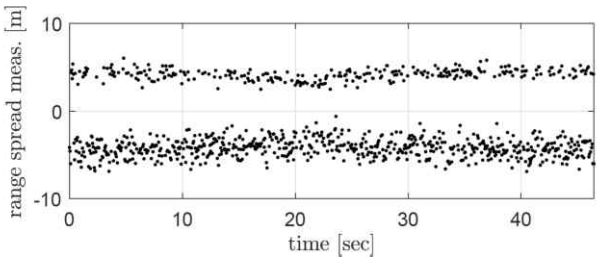


Fig. 7. Range spread measurements with the target center at 0.

in Fig. 6 is depicted as shown in Fig. 7. One of the design variables for the tracking filter, the standard deviation of the process noise is $q = 1[m/s^2]$, and the sampling period is set to 0.05 seconds.

For performance comparison, the proposed method was set against three alternative methods: the SIR (sampling importance resampling) particle filter with identical multiple modes to our proposed method (Method #1) [15], the nominal Kalman filter that performs filtering only on a single mode after merging the measurement noise PDF into a single Gaussian distribution (Method #2), and the existing approximate GSF method (Method #3). For reference, Method #3 takes the approach of approximating the modes of the *a posteriori* PDF as a single normal distribution from the perspective of MMSE at each time point. The number of particles used in the simulation for Method #1 is 10.000, and unlike the other filters, the standard deviation of the process noise was intentionally increased to $\mathrm{q} = 16$ after resampling due to frequently occurring degeneracy problems, followed by random particle generation.

The range and range rate estimation errors derived from 200 Monte-Carlo trials are depicted in Fig. 8 and Fig. 9, respectively. As can be seen in Fig. 8, the largest RMSE error occurred with Method #2, which did not account for the multiple modes of the measurement noise distribution. This is because, in Method #2, state estimates are updated using a merged measurement noise distribution with relatively large variance. When measurements are generated according to the measurement noise of the PDF that is not zero-mean, as shown in Fig. 7, it is impossible to compensate for bias.

The utility of the proposed mode merging technique can be confirmed through performance comparison with Method #3. The proposed technique achieves lower mean values of the range and range rate RMSE by approximately 0.23 $[m]$, 0.36

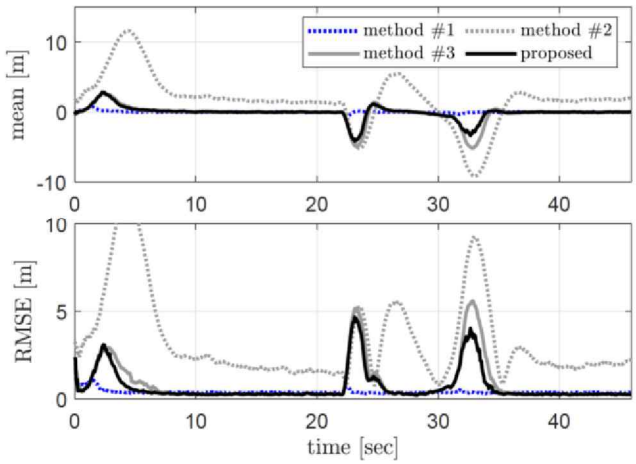


Fig. 8. Range estimation error mean and RMSE.

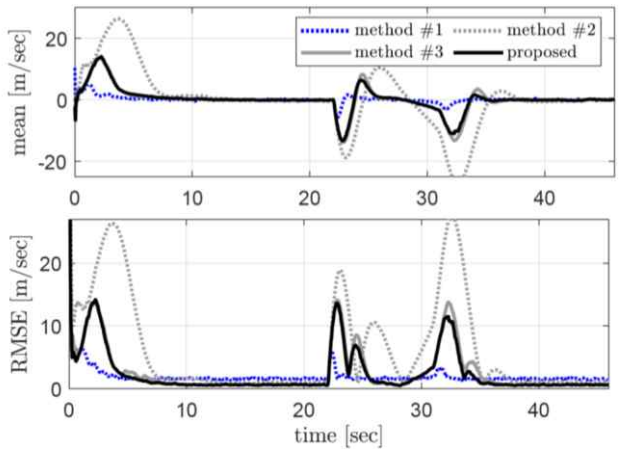


Fig. 9. Range rate estimation error mean and RMSE.

$[m/s]$, respectively, and lower peak RMSE values by about 0.93 $[m]$ and 0.57 $[m/s]$, compared to Method #3. What is especially notable are the differences in performance due to the mode merging approach, which are pronounced in the interval before the 10-second period during the filter's initial convergence and immediately after the maneuver at 22.9 seconds and 32.2 seconds.

Meanwhile, the computation time and track maintenance performance of the proposed method in comparison to the existing methods are illustrated in Fig. 10 and Fig. 11. The occurrence of degeneracy was determined based on whether the relative range error exceeded 50 $[m]$ and caused the estimates to diverge. The time required for a single measurement update of range spread measurements and system propagation computation was calculated for each method.

While Method #2 has the smallest range and range rate RMSE among the four methods, as shown in Fig. 11, about 40% of the tracks were lost within the first 10 seconds of the repeated trials due to the degeneracy problem. This is because when the particle weights are calculated using a measurement likelihood function with very small measurement noise variance, the filter prediction error increases sharply.

In terms of computation time, as can be seen in Fig. 10, it took an average of 71.38 $[ms]$, which is about 53 to 110 times more than the average computation times for the proposed method and Methods #2 and #3, which are 1.34 $[ms]$, 1.04 $[ms]$, and 0.65 $[ms]$, respectively.

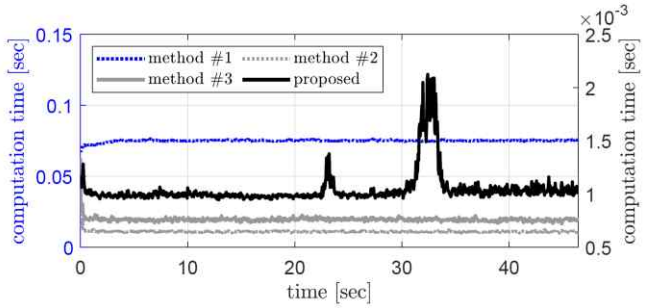


Fig. 10. Calculation time.

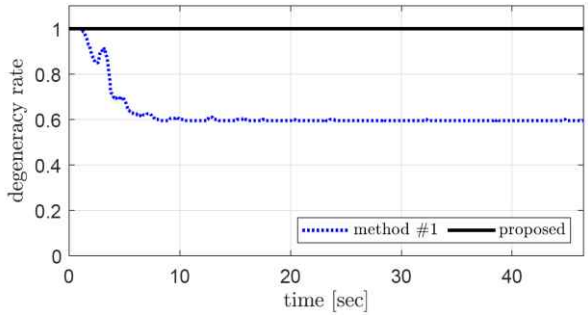


Fig. 11. Degeneracy rate.

The simulation results demonstrate that the proposed technique is a practical solution in terms of performance for BT tracking using wideband radar seekers, operational stability of the tracking filter, and computational efficiency.

## V. Conclusion

The problem of tracking ballistic targets using range spread measurements was addressed. Considering the characteristics of detections provided by a wideband radar seeker, the range spread measurement distribution was approximated by the Gaussian mixture model (GMM). Based on this result, the problem was formulated as target state estimation using GSF. A probabilistic mode merging technique was developed to solve the computational problem inherent in the conventional GSF. The proposed method not only can adaptively manage the *a posteriori* PDF even when the distribution varies the measurement with the relative geometry, but also has the advantage of high computational efficiency and easy implementation. Through simulation, it is verified that the computation time of the proposed method is reduced by more than 50 times compared to the particle filter. In addition, unlike the particle filter, the proposed algorithm does not have the degeneracy problem that causes target tracking failure. Owing to its performance and reliability, the proposed method is expected to be a practical choice for improving the hit-to-kill capability of surface-to-air missiles with a wideband radar seeker.

## Acknowledgment

This work was supported by Theater Defense Research Center funded by Defense Acquisition Program Administration under Grant UD240002SD.

## References

[1] W. S. Ra, I. H. Whang, H. S. Shin, and A. Tsourdos, "Efficient aimpoint tracking using target range profiles of a wideband FMCW seeker," *International Journal of Control, Automation and Systems*, vol. 15, pp. 1969-1974, 2017.

[2] B. Ristic, S. Arulampalam, and N. Gordon, *Beyond the Kalman filter: Particle filters for tracking applications*. Artech house, 2003.

[3] A. Kong, J. S. Liu, and W. H. Wong, "Sequential imputations and Bayesian missing data problems," *Journal of the American statistical association*, vol. 89, no. 425, pp. 278-288, 1994.

[4] Daum, F., and Huang, J., "Particle degeneracy: root cause and solution," In *Signal Processing, Sensor Fusion, and Target Recognition XX*, vol. 8050, pp. 367-377, SPIE, 2011.

[5] H.W. Sorenson and D.L. Alspach. "Recursive Bayesian estimation using Gaussian sums," *Automatica*, vol. 7, no. 4, pp. 465-479, 1971.

[6] M. L. Psiaki, , J. R. Schoenberg, and I. T. Miller, "Gaussian sum reapproximation for use in a nonlinear filter," *Journal of Guidance, Control, and Dynamics*, vol. 38, no. 2, pp. 292-303, 2015.

[7] H. Xu, H. Yuan, K. Duan, W. Xie, and Y. Wang, "An Adaptive Gaussian Sum Kalman Filter Based on a Partial Variational Bayesian Method," IEEE Transactions on Automatic Control, vol. 65, no. 11, pp. 4793-4799, 2019.

[8] A. R. Runnalls, "Kullback-Leibler approach to Gaussian mixture reduction," *IEEE Transactions on Aerospace and Electronic Systems*, vol. 43, no. 3, pp. 989-999, 2007.

[9] F. Faubel, J. McDonough, and D. Klakow, "The split and merge unscented Gaussian mixture filter," *IEEE Signal Processing Letters*, vol. 16, no. 9, pp. 786-789, 2009.

[10] G. Terejanu, P. Singla, T. Singh and P. D. Scott, "Adaptive Gaussian Sum Filter for Nonlinear Bayesian Estimation," *IEEE Transactions on Automatic Control*, vol. 56, no. 9, pp. 2151-2156, Sept. 2011.

[11] D. Alspach, , and H. Sorenson, "Nonlinear Bayesian estimation using Gaussian sum approximations," *IEEE transactions on automatic control*, vol. 17, no. 4, pp. 439-448, 1972.

[12] R. A. Singer, "Estimating optimal tracking filter performance for manned maneuvering targets," *IEEE Transactions on Aerospace and electronic systems*, vol. AES-6, no. 4, pp. 473-483, July 1970.

[13] D. Lerro and Y. Bar-Shalom, "Automated Tracking with Target Amplitude Information," *1990 American Control Conference*, 1990, pp. 2875-2880, 1990.

[14] P. L. Bogler, *Radar principles with applications to tracking systems*, New York, 1990.

[15] M. S. Arulampalam, S. Maskell, N. Gordon, and T. Clapp, "A tutorial on particle filters for online nonlinear/non-Gaussian Bayesian tracking," *IEEE Transactions on signal processing*, vol. 50, no. 2, pp. 174-188, 2002.